IOSR Journal Of Applied Geology And Geophysics (IOSR-JAGG)
E-ISSN: 2321–0990, P-ISSN: 2321–0982.Volume 12, Issue 5 Ser. I (Sept. – Oct. 2024), 27-34
Www.Iosrjournals.Org

Site Characterization In Champhai Town Area Of Mizoram State In Northeast India: Geological And Geophysical Studies

Sandipan Das[1*], Mohan Babu M[2], R Nyna Renu[2], Saralin Khongwar[3], Joe Joseph[4], Jnana Ranjan Kayal[5]

Earthquake Geology Division, Geological Survey Of India, North Eastern Region, Shillong, India
Geophysics Division, Geological Survey Of India, Southern Region, Hyderabad, India
Geophysics Division, Geological Survey Of India, Western Region, Jaipur, India
State Unit Karnataka & Goa, Geological Survey Of India, Southern Region, Bangalore, India
Formerly: Geophysics Division, Geological Survey Of India, Kolkata, India

Abstract
The Mizoram state of northeast region (NER), India located in close proximity to Indo-Burma subduction zone, recently experienced an earthquake swarm; eight severely felt earthquakes (Mw 5.0–5.9) occurred during April–October, 2020 around Champhai town that caused damages to several buildings and ground cracks with maximum reported MSK intensity VIII. The largest event Mw 5.9, at depth 15 km, occurred on April 16 (ISC catalog). The present study deals with site characterization of the Champhai town area by geological and geophysical investigations. The geological investigation involves detailed mapping of the lithounits, and the geophysical investigation includes shallow (down to 30 m) shear wave velocity (V_s^{30}) and site amplification (S_A) measurements in an about 50 sq km area in the town. Some 23 sites are selected for V_s^{30} measurements using the Multichannel Analysis of Surface Wave (MASW) technique. The observed V_s^{30} ranges from 200 m/s to 1060 m/s classifying the area into three categories: Class-B (hard rock), class-C (soft rock), and class-D (stiff soil) as per National Earthquake Hazard Reduction Program (NEHRP) guidelines. Geologically, the class B and C sites are represented by arenaceous and argillaceous Tertiary rocks, respectively, whereas the class D is represented by the Quaternary sediments. Site amplification (S_A) studies, on the other hand, are carried out by making ambient noise surveys at some 52 selected stations using a digital seismograph. The ambient noise data are analyzed by the Nakamura method of H/V spectral ratio. The overall variation of peak amplification of the sites ranges from 1.26 to 6.65. A good correlation is obtained; the observed V_s^{30} and site amplification (S_A) maps are fairly comparable with the detailed geological or lithounit map. These maps are much useful for seismic hazard microzonation of the town area to mitigate seismic hazard-risk.

Keywords: *Site characterization, multichannel analysis of surface waves (MASW), shallow shear wave velocity (V_s^{30}), site amplification (S_A), Indo-Burma subduction zone.*

Date of Submission: 03-10-2024 Date of Acceptance: 13-10-2024

I. Introduction

The whole northeast region (NER) of India is demarcated as zone V, a most seismic hazard-risk zone in the zoning map of India (BIS, 2002). The Champhai town is located in the easternmost part of the Mizoram state having international border with Myanmar to the east. Population wise Champhai is the third biggest town in Mizoram. It is linked with Myanmar by a surface road, which is the main route for Indo-Myanmar border trade, making it one of the biggest commercial centers in Mizoram. Seismically, northeast India is one of the most active regions of the world (Figure 1). The NER is jawed between two tectonic arms, Himalayan collision zone to the north and Indo-Burma atypical subduction zone to the east. It has produced two (1897 and 1950) devastating great earthquakes (Mw> 8.0), some 16 large (Mw $\geq$ 7.0) and many damaging strong earthquakes Mw $\geq$ 6.0 in the NER since the 1869 Cachar earthquake (Mw 7.4) in Assam valley (Kayal, 2008; Kayal et al, 2012). Epicenters of these events with major tectonic features are shown in Figure 1.

Recently, during April–October, 2020, Mizoram experienced a swarm activity of earthquakes; some 35 events with magnitude Mw 4.0 - 5.9, including eight events of Mw $\geq$ 5.0, occurred in and around Champai town area (Hazarika and Kayal, 2021). The largest event Mw 5.9 (depth 15 km) occurred on April 16, 2020 (ISC Catalog), and it caused damages to several buildings and ground cracks with a maximum MSK intensity VIII (Malsawma et al., 2021). Then a series severely felt seven earthquakes Mw $\geq$ 5.0 occurred at a shallower depth

(<35 km) (ISC catalog; Hazarika and Kayal, 2021), which was followed by some 27 events of Mw $\geq$ 4.0 (NCS catalog). All these events happened in the inner Indo-Burma Wedge (IBW) at the subduction zone. Seismotectonics of this sudden burst of events were reported by Hazarika and Kayal (2021) and Malsawma et al. (2021).

This sudden burst of earthquakes or swarm activity created a local panic. Thus, the Geological Survey of India (GSI) undertook a field investigation program for site characterization to assess seismic hazard-risk in this populated commercially busy town involving detailed geological and geophysical investigations in an area of about 50 sq km in the Champai town. The geological investigation involves detailed mapping of the lithounits. The geophysical investigations involve shear-wave velocity (V_S^{30}) and site amplification (S_A) measurements. Results of these investigations are highlighted here.

II. Geological Investigation

The Mizoram state is sitting over the Indo-Burma subduction zone; two major faults cut across Mizoram in N-S direction; these are the Kaladan Fault (KDF) and Churachandpur Mao Fault (CMF), (Figure 1). General geology of Mizoram is depicted by a repetitive succession of Neogene arenaceous and argillaceous sedimentary rocks belonging to the Barail, Surma and Tipam Group of Tertiary rocks folded into alternating NNE-SSW trending anticlines and synclines forming longitudinal hills and valleys in the Indo-Burma Ranges (IBR). The lithounits include mostly inter-bedded sequence of sandstone, siltstone, shale, sandy shale and at places limestone. The higher and lower grounds are occupied by arenaceous and argillaceous groups of rocks, respectively. The oldest rock unit uncovered in the region belongs to Barail Group overlain by Surma Group with a faulted contact.

A detailed geological mapping is carried out on 1:25000 scale covering the selected 50 sq km area in and around Champhai Town (Figure 2). The area exposes a thick monotonous sequence of both argillaceous and arenaceous sedimentary rocks belonging to the Barail Group of Eocene to Oligocene age represented by Laisong Formation, Kelkang Formation and the Tikak Parbat Formation having gradational contact with one another. However, in the study area the Saikahlui Fault marks the contact between Liasong and Kelkang Formation (Figure 2), (Sumanth & Esakkimuthu, 2010). This fault has been demarcated based on DEM imagery and abrupt change in slope. A thick patch of fluvial/recent Quaternary undifferentiated sediments, consisting of sand, silt and clay is present in the central portion of the study area represented by valley which is used for mainly crop cultivation, pisciculture and other agricultural plantation. The general trend of the beds within the study area is E-W and at places, swings to NE-SW, NW-SE direction, and dips range from 5° to 35°.

III. Geophysical Investigation

Shear wave velocity is a significant factor for evaluating dynamic site reaction. In site classification studies, shear wave velocity measurement down to 30 m depth (V_s^{30}) are generally considered; it provides useful information to classify the subsurface soil / rock structures (Borcherdt and Glassmoyer, 1992; Borcherdt, 1994; Anderson et al., 1996; Shafiee et al., 2006; Wen et al., 2008). The V_s^{30} generated by Multichannel Analysis of Surface Wave (MASW) are used for site characterization adhering to the National Earthquake Hazard Reduction Program (NEHRP), Building Seismic Safety Council (2001) and Uniform Building Code (UBC) (ICBO, 1994). Site amplification (S_A) study, on the other hand, provides the amplification factor of seismic waves at the locations for different geologic conditions. Site ambient noise is recorded for estimating the S_A.

MASW (V_S^{30})

In the recent past, the MASW technology is gaining significant importance in engineering geophysics, geotechnical and civil engineering projects that provides information on the physical characteristics of in-situ soils and rock formations. It involves analysis the Rayleigh waves (R-wave) on a multichannel system to get the dispersion characteristics. The shallow surface shear wave velocity (*Vs*) profiles can be constructed by investigating the dispersion feature of ground roll recorded in seismic data. Site categorization studies have made extensive use of the MASW across the globe (e.g. Park and Elrick, 1998; Xia et al. 1999; Park et al., 2002; Zhang et al., 2004; and Xu et al., 2006), and in India there has been numerous applications (e.g. Anbazhagan and Sitharam, 2008; Sil and Sitharam, 2014; Kumar et al., 2022).

A MASW weight drop method, DAQ Link 4 Seismograph data acquisition system, is used here for acquiring the data in SEGY format with the help of Vibroscope software. This study employed a roll-along technique of data collection using an active seismic source and a linear receiver array. With a linear arrangement of the geophones spaced 3 m apart, 24 geophones made up the instrument sets. The seismic waves were generated by an explosive shot fired at 10, 46, and 82 m away. The geophones picked up these waves. The shear wave velocity is calculated by processing the collected Rayleigh wave in the Geogiga seismic pro 9.02 program. When technical difficulties arose with the weight drop mechanism, sledge hammers were employed at

a few locations. There are three steps to the MASW process: (a) gathering data from the field channels, (b) calculating dispersion curves, and (c) reversing these curves to provide 1-D depth-versus-time profiles (Park, 1999). A few examples of shear wave velocity depth - profiles are illustrated in Figure 3.

Site Amplification (S_A)

In site amplification or site response investigation, we have used a Nanometrics make DAS (Data Acquisition System) of Taurus digital seismograph with Lennartz LE-3D lite tri-axial seismometer with 1 Hz natural frequency for recording seismic ambient noise. The ambient noise was recorded continuously for about 2 hours at 52 samples per second with internal GPS timing system. Site locations are marked using a handheld Garmin GPS. These data are analyzed by Nakamura (1989) method that involves H/V (Horizontal/Vertical) amplitude spectra at each location. Site amplifications mainly depend on the impedance contrast between the subsurface layers. A few representative examples of S_A (H/V) curves are also illustrated in Fig.3.

IV. Results And Discussion

Surface-waves have dispersion property; different wavelengths have different penetration depth and, therefore, transmit with different velocity. Thus, by examining the dispersion of surface waves, a near-surface velocity profile can be obtained. The selected 23 sites with minimal cultural noise were considered for dispersion curve extraction. Examples of depth profiles of shear wave velocity at a few selected sites (9, 4 and 18) over different litho-units are illustrated in Figure 3. The site 9 is situated over loose Quaternary sediments (Figure 3a), and it shows low *Vs* (150-450 m/s) down to 20 m depth, but below 20 m depth it rises from 600 to 1200 m/s (Figure 3b). The lower *Vs* in the upper part of the depth-profile may be attributed to poor compaction of the Quaternary sediments; the higher velocity (700 -800 m/s) of the bed rock at 20-30 m depth is, however, well reflected in this profile. The site 4, which is situated on sandstone of the Upper Barail (Tertiary) formation, shows moderate shear wave velocity (400-600 m / s) at 5 -7 m depth possibly due to thin soil cover / weathered layer at the top, but it attains more than 700 m/s below 7 m depth at the bed rock. The site 18, over the hard rock on the Lower Barail (Tertiary) formation, on the other hand, shows shear wave velocity 700 m/s almost from the surface. Normally, lower *Vs* (300-600 m/s) are observed for weathered rock or soft rock, and higher values (above 700 m/s) for hard rock or bed rock (e.g. Anbazhagani and Sitharam, 2009). The observations in this study clearly depict depth of the bed rocks in the area, and it varies spatially due to differing geologic conditions. The bed rock is deeper (20-25 m) below the Quaternary sediments and shallower (0-5 m) below the Tertiary formations.

In order to have coherent picture on *Vs* for 30 m column, the *Vs* values obtained at each site are time-term averaged. The time-term averaged shear wave velocity (V_s^{30}) ranges from 180 m/s to 1500 m/s in the study area; list of the MASW sites with their respective V_s^{30} values are given in Table 1. These data are then used for preparing the V_s^{30} map (Figure 4). Based on the NEHRP (BSSC, 2003) site classification (Table 2), the study area may be classified into three zones, B, C and D. The area falling under Site Class B and C are represented by arenaceous and argillaceous Tertiary rocks respectively, whereas Site Class D is represented by Quaternary sediments (Figure 2).

Site amplification (S_A) factor, a parameter which is frequency dependent and gives an estimate of degree of amplification of wave energy when it passes through the medium. The Figure 3(c) illustrates representative site amplifications S_A at the three selected sites of differing geology. Over the Quaternary loose sediments (site CH 20), we observe higher amplification (A_o 4.69) at a predominant frequency (f_o 0.76). The Upper Barail (Tertiary) sandstone (site CH 44), on the other hand, shows a higher amplification (A_o 1.36) at a predominant frequency (f_o 8.74 Hz), and interestingly a de-amplification at frequency 0.4-0.6 Hz. The Lower Barail Tertiary sandstone / siltsone (site CH 09) shows higher amplification (A_o 1.26) at a predominate frequency (f_o 4-6 Hz) and de-amplification at frequency 0.4-0.6 Hz. These observations clearly define that the hard rock Tertiary formations generate comparatively lower site amplifications (1.26-1.36) at CH 44 and CH 09, whereas the loose Quaternary sediments at the site CH 20 produce much higher amplification (4.69). Based on the site amplification data at the 53 sites, a S_A map is presented in Figure 5 with station locations.

Further, a correlation between V_s^{30} and site amplification (S_A) is examined drawing composite curves using the respective measurements at 22 common measurements sites, say within 50 m of close vicinity to each other. The V_s^{30} values are normalized (to $V_{s30}/100$) for the plot. These curves show an inverse correlation (Figure 6). This observation fairly defines that the higher the V_s^{30} (hard rock), the lower the site amplification S_A , and vice versa.

V. Conclusions

An earthquake swarm, with a largest event Mw 5.9 and MSK intensity VIII, near the Champhai town area in Mizoram state of NER, India caused some damages and created a local panic. A seismic hazard–risk evaluation study was taken up by the GSI. Along with a detailed geological mapping, geophysical

investigations (V_s^{30} and S_A mapping) were carried out in an area of about 50 sq km in the town. The surface geological map identified the differing litho-units of the Tertiary and Quaternary deposits and a fault in the area.

In geophysical investigation, the Vs depth-profiles obtained by the MASW survey reveal that below the Quaternary sediments the higher Vs (>700 m/s) bed rock is much deeper (20-25 m). In the Tertiary rock formations, on the other hand, the higher velocity bed rock is shallower (0-5 m). The V_s^{30} obtained from 23 depth-profiles are then used to prepare a V_s^{30} map that classified the area into Site class B, Site class C and Site class D as per NEHRP classification chart. The S_A investigation by noise survey at 52 locations records higher site amplifications (A_o 4–6) in the Quaternary sediments, and lower amplifications (A_o 1.2-1.3) in the Tertiary rock formations. These data are used to present a S_A map. The V_s^{30} and S_A maps are much useful for geotechnical engineering applications and urban planning to mitigate seismic hazard-risk in this populated town area.

Ethical statement: The authors declare that they have no known competing financial interests or personal relationships that could have appeared to influence the work reported in this article. This material is the authors' own original work, which has not been previously published elsewhere. The paper properly credits the meaningful contributions of co-authors and co-researchers

Acknowledgement

The authors are thankful to Director General, GSI; Addl. Director General & HoD, GSI, NER; DDG & RMH-IV, GSI, NER for providing the necessary support to carry out the work. The Director, Earthquake Geology Division, GSI, NER is acknowledged for providing all support and encouragement to prepare this manuscript.

References

[1] Anbazhagan, P. And Sitharam, T. G. (2008): Site Characterization And Site Response Studies Using Shear Wave Velocity Journal Of Seismology And Earthquake Engineering 10(2) P 53–67.
[2] Anbazhagan, P. Sitharam, T. G. (2009): Spatial Variability Of The Depth Of Weathered And Engineering Bedrock Using Multichannel Analysis Of Surface Wave Method. Pure Appl. Geophysics, 166(3), 409–428, Doi: 10.1007/S00024-009-0450-0
[3] Anderson, J.G., Lee, Y., Zeng, Y. And Day, S. (1996): Control Of Strong Motion By The Upper 30 Meters, Bulletin Of The Seismological Society Of America, V.86, Pp: 1749-1759.
[4] Borcherdt, R. D. And Glassmoyer, G. (1992): On The Characteristics Of Local Geology And Their Influence On Ground Motions Generated By The Loma Prieta Earthquake In The San Francisco Bay Region, California, Bulletin Of The Seismological Society Of America, V.82, Pp: 603-641.
[5] Borcherdt, R.D. (1994): Estimates Of Site-Dependent Response Spectra For Design (Methodology And Justification). Earthquake Spectra V.10, Pp: 617– 653.
[6] Bssc (2003) Nehrp Recommended Provisions For Seismic Regulations For New Buildings And Other Structures (Fema 450), Part 1: Provisions, Building Seismic Safety Council For The Federal Emergency Management Agency (Report Fema 368), Washington, Dc.
[7] Hazarika, D. And Kayal, J. R. (2021): Recent Felt Earthquakes (Mw 5.0–5.9) In Mizoram Of North-East India Region: Seismotectonics And Precursor Appraisal. Geological Journal, 2022; 57:877–885, Doi: 10.1002/Gj.4290.
[8] Kayal, J.R (2008): Microearthquake Seismology And Seismotectonics Of South East Asia(P. 503). The Netherlands/India: Springer/Capital Pub Co.
[9] Kayal, J. R., Arefiev, S. S., Baruah, S., Hazarika, D., Gogoi, N., Gautam, J. L., Baruah, S. (2012): Large And Great Earthquakes In The Shillong Plateau - Assam Valley Area Of Northeast India Region: Pop-Up And Transverse Tectonics. Tectonophysics, 532–535, 186–192. Https://Doi.Org/ 10.1016/J.Tecto.2012.02.007.
[10] Kumar, A., Satyannarayana, R., Rajesh, B. G. (2022): Correlation Between Spt-N And Shear Wave Velocity (V_s) And Seismic Site Classification For Amaravati City, India. Journal Of Applied Geophysics, V.205, Doi: 10.1016/J.Jappgeo.2022.104757
[11] Malsawma, J., Lalnuntluanga, P., Sailo, S., Vanthangliana, V., Tiwari, R.P. And Gahalaut, V.K. (2021): The 22 June 2020. Mizoram, India Earthquake (Mw 5.5): An Unusual Intra-Wedge Shallow Earthquake In The Indo Burmese Wedge. Current Science. 120 (9): 1514-1516.
[12] Nakamura, Y. (1989): "A Method For Dynamic Characteristics Estimation Of Subsurface Using Microtremor On The Ground Surface", Quaterly Reports Of The Railway Technical Research Institute 30, 25-33
[13] Park, S. And Elrick, S. (1998): Predictions Of Shear-Wave Velocities In Southern California Using Surface Geology. Bulletin Of The Seismological Society Of America, V.88, Pp: 677-685.
[14] Park, C.B., Miller, R.D., And Xia, J. (1999): Multichannel Analysis Of Surface Waves (Masw). Geophysics, V.64, Pp: 800–808.
[15] Park, B. C., Miller, D. R. And Miura, H. (2002): Optimum Field Parameters Of An Masw Survey, Seg-J, Tokyo, May 22-23, 2002.
[16] Shafiee, A., And Azadi, A. (2006): Shear-Wave Velocity Characteristics Of Geological Units Throughout Tehran City, Iran. Journal Of Asian Earth Sciences.
[17] Sil, A. And Thallak, S. G. (2014): Comprehensive Seismic Hazard Assessment Of Tripura And Mizoram States. Journal Of Earth System Science 123(4):837-857, Doi: 10.1007/S12040-014-0438-8
[18] Sumnath, J. N. And Esakkimuthu, T. (2010): Report On Specialised Thematic Mapping Along Bungzung And Laisomual Hill Ranges, Champhai District, Mizoram, Unpublished Gsi Report Fsp 2007-08 & 2008-09.
[19] Wen, R., Shi, D., And Ren, Y. (2008): Site Classification Based On Geological Genesis And Its Application. The 14th World Conference On Earthquake Engineering, Beijing, China.
[20] Xia, J., Miller, R.D., And Park, C.B. (1999): Estimation Of Nearsurface Shear Wave Velocity By Inversion Of Rayleigh Waves. Geophysics, V.64, Pp: 691-700.

[21] Xu, C. And Butt, S. D. (2006): Evaluation Of Masw Techniques To Image Steeply Dipping Cavities In Laterally Inhomogeneous Terrain. Journal Of Applied Geophysics, V.59, Pp: 106-116.
[22] Zhang, S.X., Chan, L.S., And Xia, J. (2004): The Selection Of Field Acquisition Parameters For Dispersion Images From Multichannel Surface Wave Data. Pure Application Geophysics (161):185-201.

Table 1 List of MASW sites with respective V_s^{30} values

MASW Location	Long	Lat	Vs30 m/s	Location
1	93.3430	23.4792	514.5	Tlangnuam area
2	93.3361	23.4955	801.5	Hmunmeltha
3	93.3121	23.4858	504.5	Vengsang
4	93.3114	23.4993	625.4	Hmunmeltha
5	93.3455	23.4346	547.9	Ruantlang
6	93.3576	23.4493	1060.3	Maulnuam-Tiau road
7	93.3472	23.4529	921.8	Maulnuam
8	93.3262	23.4619	739.1	KV school Dinthar
9	93.3531	23.4678	328.8	New Champhai
10	93.3600	23.4803	905.9	Tlangsam
11	93.3454	23.4737	489.2	Tlangsam
12	93.3313	23.4687	568.6	Kanan
13	93.3150	23.4714	669.4	Behind PHE office
14	93.3168	23.4568	764.7	Jail Veng
15	93.3327	23.4233	447.8	Maulkawi
16	93.3232	23.4400	505.4	Mup Park
17	93.3420	23.5002	492.4	Zote
18	93.3416	23.4417	749.5	Ruantlang
19	93.3399	23.4606	203.4	Maulnuam
20	93.3250	23.4928	622.1	Hmunmeltha
21	93.3277	23.5060	571.5	Hmunmeltha
22	93.3612	23.5003	472.8	Zote
23	93.3263	23.4828	596.2	Bethel Veng

Table 2 Site classification based on V_s^{30} values (NEHRP site classification, BSSC 2003)

Site class	**Description**	**Vs30 (m/sec)**
A	Hard rock	>1500
B	Rock	760-1500
C	Very dense soil & soft rock	360-760
D	Stiff soil	180-360
E	Soft clay soil	<180
F	Soils requiring additional response	NA

Figure Captions:

Figure 1: Seismicity map of the NER, India showing major tectonic features (modified from Kayal et al. (2012)). The seismic data (≥ 6 Mw) for the period 1906-2022 and (5-5.9Mw) for the period 2000-2023 are shown (source: USGS, NCS & ISC-EHB catalogue). The epicenters and magnitudes of the 1869 large and two (1897 and 1950) great earthquakes are taken from (Kayal et al., 2012). The recent three strong earthquakes (2009, 2016 and 2021) are shown by black stars. Major tectonic features; BRV: Brahmaputra River Valley, CCF: Chittagong Coastal Fault, CMF: Churachandpur-Mao Fault, DF: Dauki Fault; SF: Sylhet Fault, DhF: Dudhnoi Fault, DsT: Disang Thrust, DT: Dapsi Thrust, EBT: Eastern Boundary Thrust, KDF: Kaladan Fault, KF: Kopili Fault, LT: Lohit Thrust, MBT: Main Boundary Thrust, MCT: Main Central Thrust, MH: Mikir Hills, MT: Mishmi Thrust, NT: Naga Thrust, OF: Oldham Fault, SP: Shillong Plateau, SW: Siang Window, TFB: Tripura Fold Belt, TT: Tidding Thrust, WF: Walong Fault. (Inset: Seismic zoning map of India showing the NER of India).

Figure 2: Detailed geological map of the study area. Three representative MASW sites are shown (see text). Inset: Spatial distribution of seismicity in Mizoram (1990-2023) showing the earthquake swarm (April-October 2020) within the red enclave.

Figure 3: (a) Pictures of the three representative sites with differing geology (see Fig.2), (b) shear wave velocity depth-profiles and (c) the respective H/V curves at these three sites, respectively.

Figure 4: V_s^{30} map of the study area with the MASW site locations. The observed V_s^{30} and NEHRP site classifications are shown.

Figure 5 Site amplification (S_A) map of the study area with site locations.

Figure 6 Composite curves showing correlation between V_{s30} and site amplification at 22 sites where both the measurements are taken at close vicinity

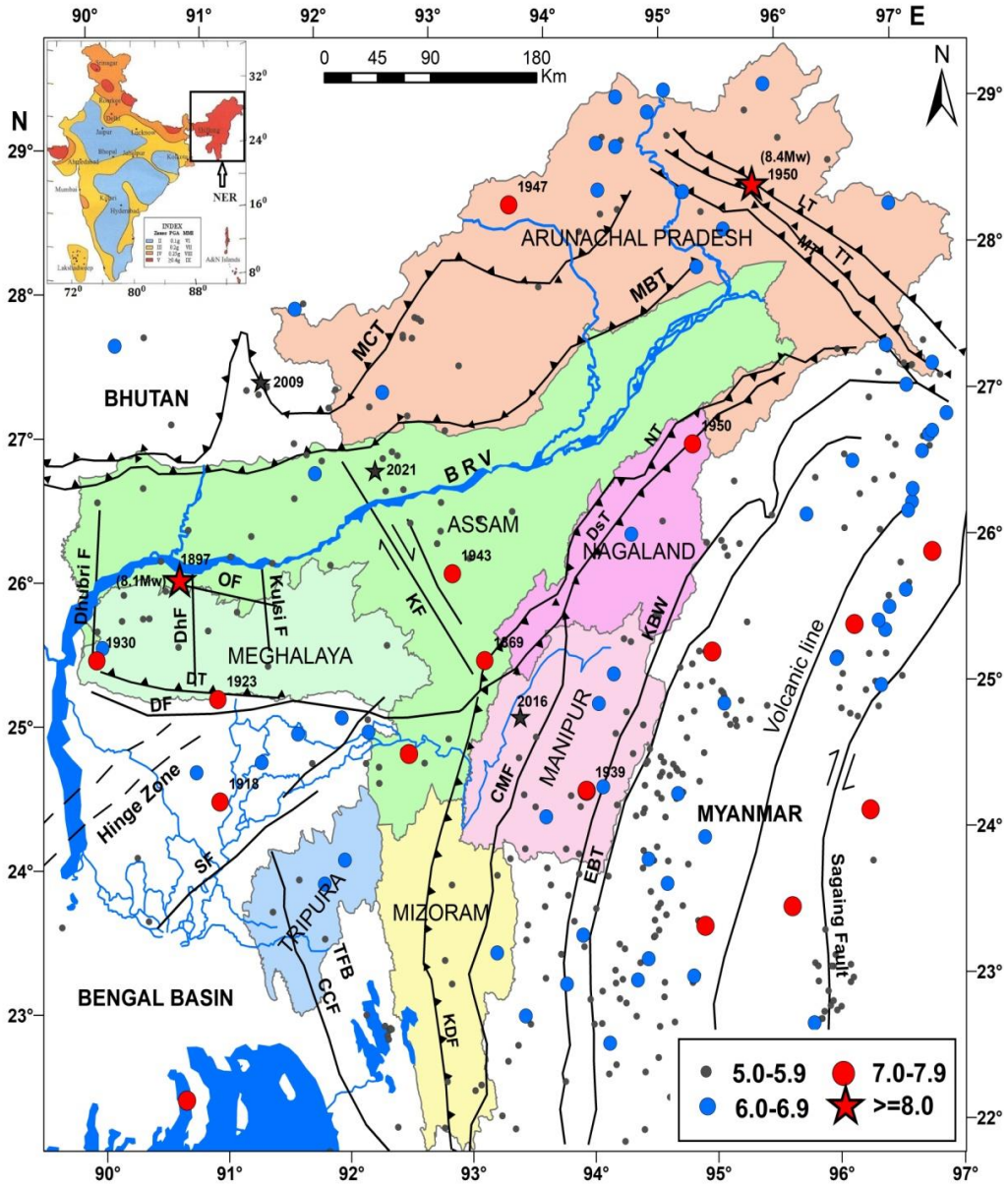

Figure 1 Seismicity Map Of The NER, India Showing Major Tectonic Features (Modified From Kayal Et Al. (2012)). The Seismic Data (≥ 6 Mw) For The Period 1906-2022 And (5-5.9Mw) For The Period 2000-2023 Are Shown (Source: USGS, NCS & ISC-EHB Catalogue). The Epicenters And Magnitudes Of The 1869 Large And Two (1897 And 1950) Great Earthquakes Are Taken From (Kayal Et Al., 2012). The Recent Three Strong Earthquakes (2009, 2016 And 2021) Are Shown By Black Stars. Major Tectonic Features; BRV: Brahmaputra River Valley, CCF: Chittagong Coastal Fault, CMF: Churachandpur-Mao Fault, DF: Dauki Fault; SF: Sylhet Fault, Dhf: Dudhnoi Fault, Dst: Disang Thrust, DT: Dapsi Thrust, EBT: Eastern Boundary Thrust, KDF: Kaladan Fault, KF: Kopili Fault, LT: Lohit Thrust, MBT: Main Boundary Thrust, MCT: Main Central Thrust, MH: Mikir Hills, MT: Mishmi Thrust, NT: Naga Thrust, OF: Oldham Fault, SP: Shillong Plateau, SW: Siang Window, TFB: Tripura Fold Belt, TT: Tidding Thrust, WF: Walong Fault. (Inset: Seismic Zoning Map Of India Showing The NER Of India).

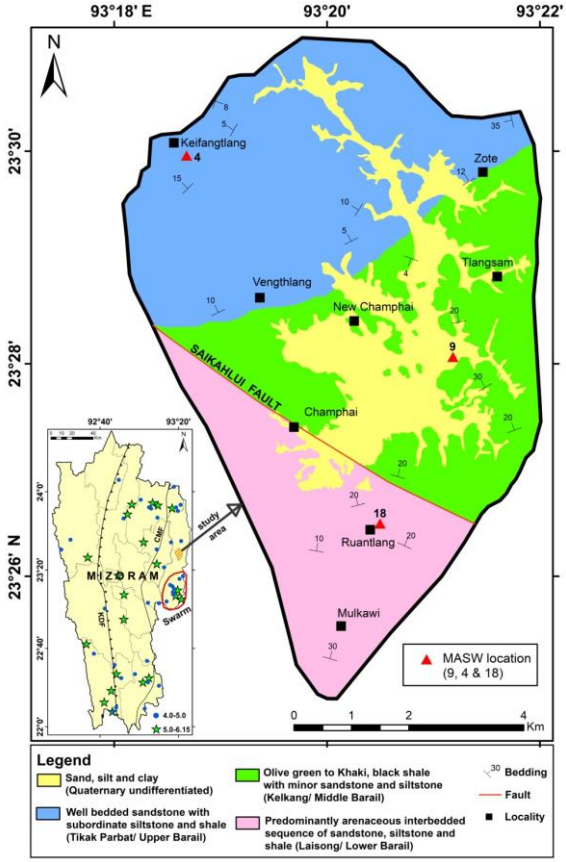

Figure 2 Detailed Geological Map Of The Study Area. Three Representative MASW Sites Are Shown (See Text). Inset: Spatial Distribution Of Seismicity In Mizoram (1990-2023) Showing The Earthquake Swarm (April-October 2020) Within The Red Enclave.

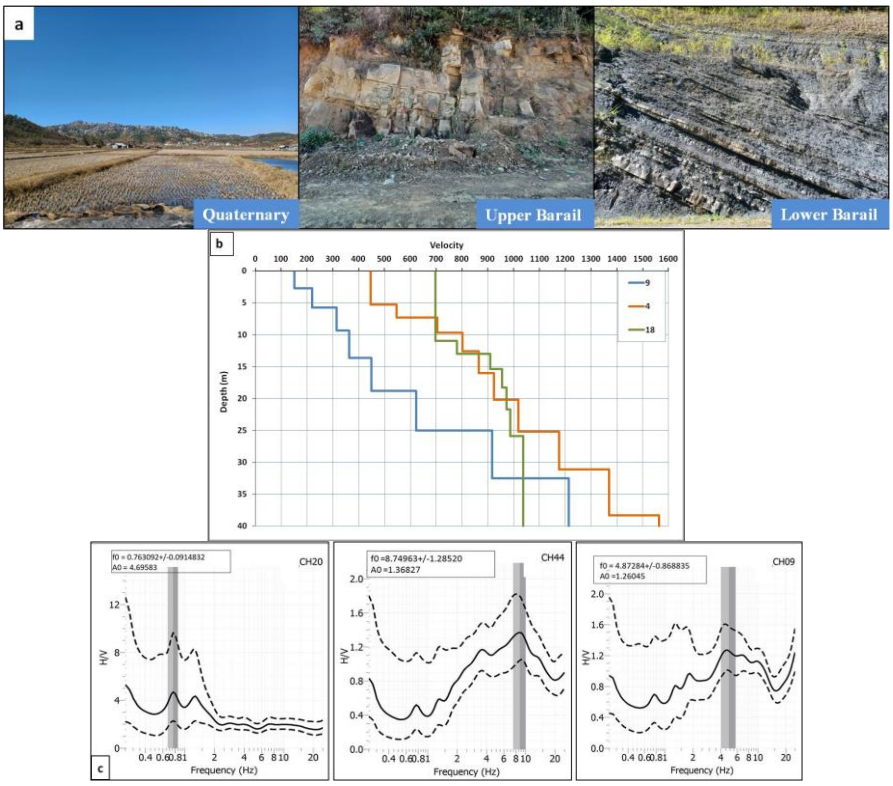

Figure 3 (A) Pictures Of The Three Representative Sites With Differing Geology (See Fig.2), (B) Shear Wave Velocity Depth-Profiles And (C) The Respective H/V Curves At These Three Sites, Respectively.

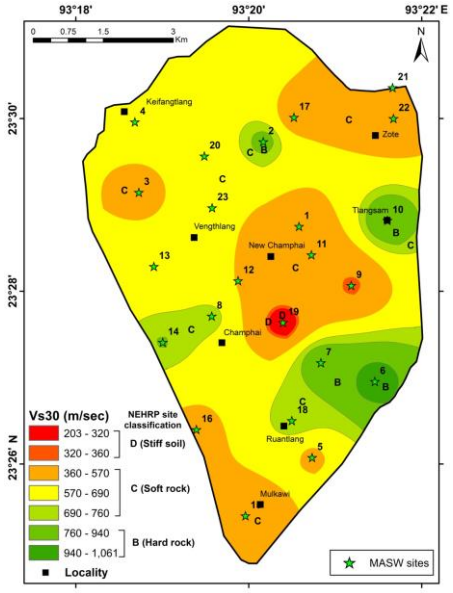

Figure 4 Vs30 Map Of The Study Area With The MASW Site Locations. The Observed Vs30 And NEHRP Site Classifications Are Shown.

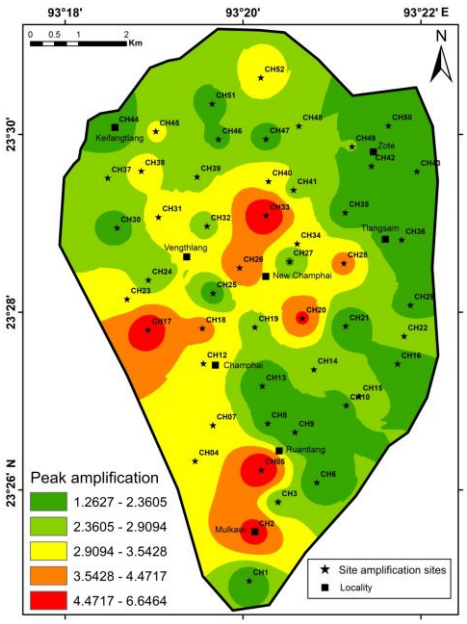

Figure 5 Site Amplification (S_A) Map Of The Study Area With Site Locations

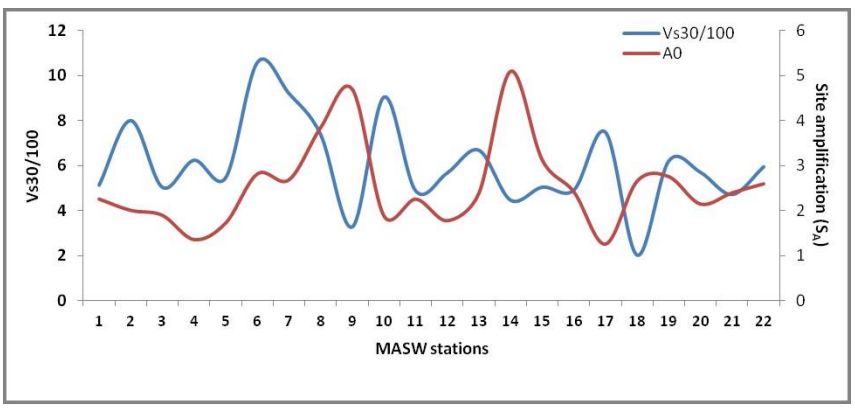

Figure 6 Composite Curves Showing Correlation Between V_s^{30} And Site Amplification At 22 Sites Where Both The Measurements Are Taken At Close Vicinity.